Tele-Impedance: Preliminary Results on Measuring and Replicating Human Arm Impedance in Tele Operated Robots

A. Ajoudani, N. G. Tsagarakis, and A. Bicchi

Abstract— **This work introduces the concept of Tele-Impedance as a method for controlling/teleoperating a robotic arm in contact with the environment. Opposite to bilateral force-reflecting teleoperation control approach, which uses a position/velocity command combined with force feedback from the robot side, Tele-Impedance enriches the command sent to the slave robot by combining the position reference with a stiffness (or full impedance) reference. The desired stiffness profile is directly estimated from the arm of the human operating the remote robotic arm. We preliminarily investigate the effectiveness of this method while teleoperating a slave robotic arm to execute simple tasks. The KUKA light weight robotic arm is used as the slave manipulator. The endpoint (wrist) position of the human arm is monitored by an optical tracking system while the stiffness of the human arm is estimated from the electromyography (EMGs) signal measurements of four flexor-extensor muscle pairs, in real-time. The performance of Tele-Impedance control method is assessed by comparing the results obtained while executing a peg-in-hole task, with the slave arm under i) constant low stiffness, ii) constant high stiffness or iii) under Tele-Impedance control. The experimental results demonstrate the effectiveness of the Tele-Impedance control method and highlight its potential use to safely execute tasks with uncertain environment constraints which may result in large deviations from the commanded position trajectories.**

I. Introduction

Over the past decades, applications of robots in unstructured and hostile for human environments have seen an intensive use of Master-Slave teleoperation systems often based on feedback sensory data.

In these systems, a human operator executes a task by controlling a manipulator (Slave) located in the remote environment using a robotic interface (Master) located at the human site. The execution of the remotely performed task is usually assisted by feeding back to the master and human operator kinesthetic feedback conveying information about the force interaction between the slave robot and the remote environment. Although these bilaterally controlled teleoperated systems outperforms the pure position controlled systems, latencies in the communication channel between the master and slave robot may generate serious issues related to the stability of the bilateral teleoperation system [1-4].

To guarantee the stability of the bilateral teleoperation system in the presence of time delays several control schemes have been proposed [4–9]. Although these techniques have demonstrated good results, especially in the case of small and fixed time delays, in many cases the stable contact and task execution is achieved through a compromise with the transparency of the system. In particular, the application of high damping actions at the master device [10-12] can generate forces which are superimposed to the forces fed back from the remote slave robot reducing the transparency of the teleoperation system.

Despite the results and continuous improvements in the control and the stability of bilateral controlled teleoperation systems, there are still many tasks in which stability and reduced transparency, if not mere cost of sensing and actuating reflected forces, prevents application of bidirectional teleoperation. Tasks which are normally performed by humans without difficulty such as drilling, reaming, chipping and many others with large uncertainly in the environment constraints, cannot be easily conducted under sensory feedback based teleoperation control. This is not only due to the stability and transparency issues mentioned above but also in many cases due to inadequate or low quality sensory information (such as position, force, velocity) which defines the mechanical work exchanged during the interaction of the teleoperated tool and the remote environment [13].

In the past decade, the introduction of torque controlled robots which can regulate actively their stiffness or full impedance properties by active control techniques [14] as well the recent developments of actuation systems which inherently integrate physical principles such as variable stiffness and damping [15-18] created new possibilities in the control of teleoperated machines and the execution of remotely conducted tasks.

It is well known for example that humans are actively regulating their arm impedance [19-23] during the execution of the task. This allows the human arm to demonstrate a versatile and stable behavior while interacting with environments with dynamic uncertainties and stochastic disturbances. It is believed that this superior capability of the human arm relies on the endpoint impedance regulation, commanded by the central nervous system, and particularly described and modeled by two different approaches (equilibrium point hypothesis [19] and internal models [20]).

Electromyography signals are considered as the best candidates to provide an insight into the overall

A. Ajoudani and A. Bicchi are within Interdepartmental Research Centre "E. Piaggio", Faculty of Engineering, University of Pisa, and within the Dept. of Advanced Robotics, Istituto Italiano di Tecnologia, Via Morego 30, 16163, Genova, Italy (e-mails: arash.ajoudani@iit.it; bicchi@centropiaggio.unipi.it).

N. G. Tsagarakis is within the Dept. of Advanced Robotics, Istituto Italiano di Tecnologia, Via Morego 30, 16163, Genova, Italy (e-mail: nikos.tsagarakis@iit.it).

biomechanical behavior of the arm since they dictate patterns of activations, regulated by CNS. It has been shown that surface electromyography signals are highly correlated with joint stiffness and the corresponding generated muscle tensions [21] and [24-26]. EMGs have been also recruited in order to map the human arm and hand movements on the robots and prosthetic devices [24, 25] and shown to have acceptable performance in classification of movements, particularly in robotic hands. However, when the continuous movement of the joints is required, highly sophisticated signal processing approaches should be applied to the segments of EMG signals which inevitably introduce latency and increase the complexity of the scheme, particularly in real time applications.

Inspired by the superior interaction performance of the human arm achieved through the regulation of its endpoint impedance, this paper proposes the use of Tele-Impedance control as an alternative method to unilateral position based control or bilateral force reflecting control during teleoperated tasks. The novelty of the proposed Tele-Impedance control method is that it provides the slave robot with additional information compared to pure position data traditionally sent to the slave robot during teleoperation. This enriched command profile considers not only the reference position data but also the impedance command profile required by the particular task. This combined command reference (position and impedance) is finally executed from the slave teleoperated robotic arm by means of accurate local controllers [29].

In the Tele-Impedance control scenario presented in this work, the human operator moves his arm in space to guide the remotely located robot to perform a pre-defined task (Peg in Hole in this work). The slave robot performs the task by tracking both the reference position profile (which corresponds to the end-point position of the arm of the human operator as measured from an optical position tracking system) and the end-point stiffness profile (estimated from the muscular activity of the operator's arm) in real-time.

The paper is structured as follows; section II presents the model of the stiffness of the human arm and the calibration procedures used. Section III presents the experimental setup used for the execution of a Peg in Hole task using the Tele-Impedance control. Experimental results for the stiffness estimation as well as data from the execution of the Peg in Hole task using the Tele-Impedance concept are introduced in section IV. Finally section V addresses the conclusions.

II. ESTIMATION OF HUMAN ARM STIFFNESS

A. Stiffness as a Model of Co-Contractions

It has been shown that the humans are able to change the size of the endpoint stiffness ellipse, whereas the orientation and shape modifications meet changes in posture [21-23, 26]. This phenomenon refers to the capability of CNS to regulate the stiffness of the joint in its equilibrium angle independent from the generated torque/force through the coactivation of antagonistic muscle pairs. Considering this, teleoperated tasks could be accomplished while adjusting coactivations and corresponding endpoint stiffness profile. For this reason, it is reasonable to consider the indexes of co-contractions for the purpose of estimation of human endpoint stiffness.

Rectified surface electromyography highly correlates with the static and dynamic stiffness and the generated muscle tensions. This nonlinear behavior is due to the nonlinear length and velocity dependency of the generated muscle tensions which clarifies nonlinear connection between muscle tensions and generated surface EMGs, However, in this work, this behavior is assumed linear and moment arms are considered constant around the task space (close to isometric conditions). Although this simplification may introduce precision errors in the estimation of the human arm stiffness it is still valid for the Tele-impedance experiment of this work as the Peg in Hole task does not require very precise estimation of the dynamic end-point stiffness.

For this reason, the proposed index of muscle co-contractions in [21] was considered to monitor the elastic behavior of human arm endpoint in task space. Based on the proposed index, the endpoint torque can be expressed by the difference between extensor and flexor moments generated as a result of the concurrence between arm extensor and flexor muscles (Eq. 1).

$$\begin{aligned} f_{ex} &= \sum_{i=1}^{n} \alpha_i . f(EMG_{ago-i}) - \sum_{j=1}^{n} \beta_j . f(EMG_{anta-j}) \\ f_{ey} &= \sum_{i=1}^{n} \alpha'_i . f(EMG_{ago-i}) - \sum_{j=1}^{n} \beta'_j . f(EMG_{anta-j}) \\ f_{ez} &= \sum_{i=1}^{n} \alpha''_i . f(EMG_{ago-i}) - \sum_{j=1}^{n} \beta''_j . f(EMG_{anta-j}) \end{aligned} \quad (1)$$

Here, f_{ex}, f_{ey} and f_{ez} denote the generated forces at the human arm endpoint in x, y and z directions, respectively. $f(EMG_{ago})$ and $f(EMG_{anta})$ are pre-processed agonist and antagonist EMG signals and coefficients ($\alpha, \beta, \alpha', \beta', \alpha''$ and β'') are all constants to be estimated. These last parameters incorporate information such as the moment arm, conversion factor from muscle activity to muscle tension and Jacobian coefficients of the transformation kinematics. Considering now the proportionality of the muscle stiffness to the muscle torque [26], an index for the measurement of human arm endpoint stiffness can be the summation of the absolute values of the generated muscle torques [21].

$$\begin{aligned} K_{xx} &= \sum_{i=1}^{n} |\alpha_i| . f(EMG_{ago-i}) + \sum_{j=1}^{n} |\beta_j| . f(EMG_{anta-j}) \\ K_{yy} &= \sum_{i=1}^{n} |\alpha'_i| . f(EMG_{ago-i}) + \sum_{j=1}^{n} |\beta'_j| . f(EMG_{anta-j}) \\ K_{zz} &= \sum_{i=1}^{n} |\alpha''_i| . f(EMG_{ago-i}) + \sum_{j=1}^{n} |\beta''_j| . f(EMG_{anta-j}) \end{aligned} \quad (2)$$

Here, K_{xx}, K_{yy} and K_{zz} denote endpoint stiffness of the human arm. Although the generalization of the above within the arm workspace can inevitably lead precision/estimation

errors, since conducted task will be accomplished in the vicinity of the posture in which the parameters are estimated and calibrated, the overall approach can still provide us with the insightful outline of the generated endpoint stiffness profile. In this work, the generated stiffness in horizontal plane is calibrated by means of direct measurements described below in model calibration section.

B. Stiffness Model Calibration

For the purpose of the calibration of the stiffness model described by Eq. (2) we performed two experiments which are described below. In these experiments one healthy subject participated. In the first experiment the subject (male; age 27) was seated on a chair, while his shoulders were restrained by two belts and his arm was supported by a rope attached to the ceiling. A spherical joint were designed and fabricated in order to reduce undesired generated torques by the subject's wrist (Figure 1. B). The joint was equipped with a 6 axis force-torque sensor (ATI-Mini-45). Using only visual feedback and under isometric conditions the subject was asked to apply and sustain on the handle a force of 5, 10 and 20 N along 8 directions in the horizontal plane and along the ±Z directions.

During the execution of this trial, EMGs from eight muscles (Figure 1. A) were acquired by means of surface electrodes (Delsys-Bangoli-16 from (Delsys Inc.)). The signals were filtered [Band-pass, 20 Hz (low) and 450 Hz (high)], sampled at 2 KHz (PCI-6220, National Instruments,), full rectified, low-pass filtered [Butterworth, cutoff frequency 2.4Hz] and normalized to the maximum voluntary contraction values in order to have signals analogous to muscle activations.

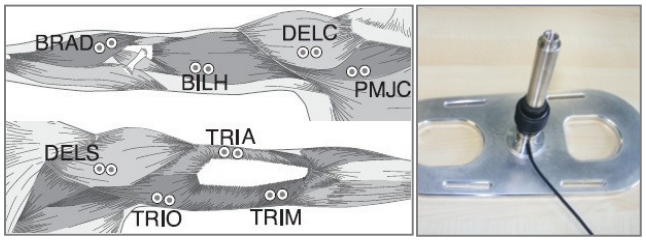

(A) (B)

Fig. 1. A. Electrode positions in EMG measurements. The eight muscles considered are: shoulder monoarticular muscles (deltoid clavicular part (DELC), pectralis major clavicular head (PMJC; flexor) and the deltoid-scapular part (DELS; extensor)), shoulder-elbow double-joint muscles (the biceps long head (BILH; flexor) and triceps long head (TRIO; extensor)) and elbow monoarticular muscles (brachioradialis (BRAD ; flexor), triceps lateral head (TRIA) and triceps medial head (TRIM; extensor)), and B. The instrumented spherical joint used during the experiment.

The human arm endpoint force was disintegrated into eight muscle activations and as a result, the parameters of Eq.1. were estimated based on 60 trials by means of least-square-error method. Then, the absolute values of these parameters were utilized for interpretation of co-contraction based index of endpoint stiffness profile as in Eq.2. Following this first estimation, a second experimental procedure based on mechanical perturbations was used in order to assess and further calibrate the stiffness model.

Stiffness estimation by means of perturbations was first proposed by [27]. Modified method was used for the estimation of inertial and viscous parameters in addition to stiffness by [22, 23].

In [22], endpoint dynamics of the human arm were modelled by four different mathematical equations; however, results demonstrate that the second order linear impedance model fits perfectly to the overall dynamics for small perturbations around an equilibrium posture (Eq. 3).

$$M\ddot{X}(t) + B\dot{X}(t) + K(X(t) - X_{eq}) = -F(t)$$
$$X(t) = \begin{bmatrix} x(t) \\ y(t) \end{bmatrix} \quad and \quad F(t) = \begin{bmatrix} f_x(t) \\ f_y(t) \end{bmatrix} \tag{3}$$

Where M, B and K are Cartesian impedance matrixes of the mass, damping and stiffness at equilibrium position X_{eq}. F(t) and X(t) are the forces and displacements of the hand in x and y directions, respectively.

In this work the KUKA light weight robotic arm (KUKA/DLR) was used to apply position perturbations with amplitude of 8 to 12 millimeters in 8 random directions in horizontal plane to the subject's hand while seating with a static posture identical to former experiments. The duration of each perturbation was approximately 300 ms. This perturbation profile assures elimination of any significant influence of voluntary reaction on the measured F/T values. Nevertheless, influences of reflex gains in impedance estimations will be compulsory due to the hardware limitations mainly due to perturbation duration constraint. A six axis F/T sensor (ATI Mini-45) was mounted at the end-effector of the KUKA robotic arm for the measurements of the restoring forces.

The displacements of the human arm at the endpoint (level of the wrist) along with shoulder and elbow positions were tracked (resolution: 0.02 mm) by Optitrack system (Natural Point Inc). The interface between the KUKA controller, the EMG acquisition board, the Optitrack position streaming data and the six axis F/T sensor in calibration experiment and real-time Tele-Impedance experiments was developed in Microsoft Visual C++ environment. The robot's position and joint/Cartesian stiffness commands were sent to the KUKA controller using the DLR's Fast Research (FR) Interface [28].

Position and force measurements were performed at a sample frequency of 200 Hz while the EMG acquisition and processing was performed at a frequency of 1 KHz. All the acquired force/torque and position measurements were filtered [Butterworth, low-pass, cutoff frequency 15 Hz] to eliminate high frequency noise. The velocity and acceleration of the human arm endpoint were calculated based on robust numerical derivative methods by means of Matlab toolboxes (The Math Works, Inc.). Acquired forces along with arm's endpoint displacements, velocity and accelerations from all trials were fit to the arm dynamics around equilibrium point as described in (3) by means of least-squared-error methods. Estimation constraints were taken into account from former studies on human endpoint impedance [22, 23]. The resulting stiffness matrix which consists of Cartesian stiffness values was then used for the

calibration of stiffness values, generated from the activation based stiffness model presented in the previous section.

The resulting scaling coefficients in x and y direction were directly calculated from real values of the arm's endpoint stiffness while their average was intentionally used for the calibration of stiffness in Z direction. Although this assumption will make us diverge from real stiffness value of the human arm endpoint in Z direction, at the same time, it permits the regulation of the stiffness in this direction, by means of co-contractions and makes it practically applicable. It is important to note here that the major hinder for the measurements of the human endpoint stiffness in 3D is the hardware limitation for the gravity compensation in Z direction, however, one of the future goals of this research group is to increase accuracy of impedance estimations in 3D by means of a currently under design manipulandum.

III. Tele-Impedance Experiment

The evaluation of the Tele-Impedance control method was performed using a classic Peg-in-Hole experiments. This task has been extensively used as a test case for spatial planning with uncertainties. Force and impedance control approaches have been used in many works in the past to cope with the dynamic interactions between the peg and the hole surfaces. In this work, the task is performed while the optimized control system called human arm is in charge of the motion planning and the regulation of the end-effector impedance of the remotely teleoperated slave manipulator.

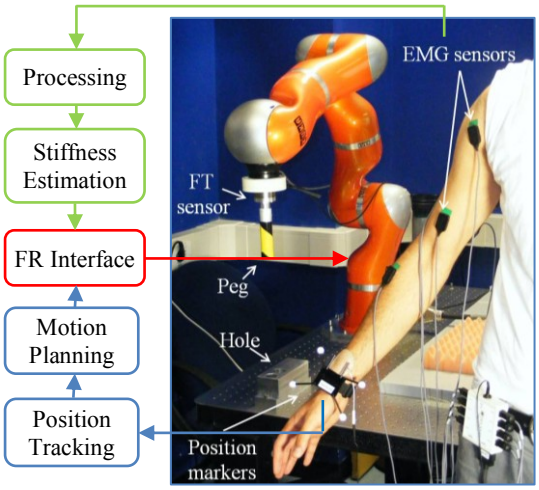

Fig. 2. Experimental setup. KUKA light weight robotic arm, EMG electrodes, peg, hole, position tracking markers and F/T sensor are shown in picture.

The experimental setup and information flow are shown in Fig 2. Rigid body markers were attached to the wrist, elbow and shoulder of human arm to track the humans arm motion, however, the only data, used for the motion planning and reference trajectory calculation was the human arm endpoint path (wrist level). At the same time, EMG signals were acquired for the purpose of the human arm endpoint stiffness calculations based on the activation based stiffness model described in the previous section. All processing and control algorithms were performed in real-time. Software interfaces, sampling frequencies, and hardware specifications are identical to those reported in the previous sections.

Motion Planning: KUKA's base frame was considered as the reference frame and all other frames (Optitrack and FT sensor frames) were conformed to this reference frame. Position path of the human wrist was measured, filtered [low-pass, cutoff 15Hz] and used for the trajectory planning.

The FR Interface was utilized for commanding the position and Cartesian impedance controllers of the KUKA arm. Incremental position references were sent to KUKA calculated from the position tracking errors in three dimensions (Eq. 4). This approach was taken into account to cope with the drift problem and tracking inaccuracy due to the delay between reference commands and generated movement in KUKA's end-effector.

$$e_\xi = \xi_h - \xi_k \qquad \xi = [x \quad y \quad z] \tag{4}$$

Where e is the three dimensional tracking error vector between the reference Cartesian position of human wrist ξ_h, and the current Cartesian position of KUKA's end-effector, ξ_k.

Impedance Control: It has been shown in [21] that the EMG based stiffness model, is valid for small movements around the static posture, which the parameters were estimated and calibrated. Considering this, the correspondence between the robot arm posture and the pose of the human arm was selected in a way that when the peg is just above the hole surface and almost aligned with the hole the corresponding human arm posture is in the vicinity of the arm configuration used for the estimation and calibration of the stiffness model. Once the peg is aligned with the hole, the operator adjusts the stiffness values by means of increased co-contractions and performs the peg insertion. The increased co-contractions are required in order to overcome the frictional forces between the surfaces of the peg and the hole during the insertion. Low co-contractions result in low end-effector stiffness on the KUKA arm which prevents the full insertion of the peg. Therefore the operator has to increase the coactivations until the KUKA's end effector elastic profile crosses the lower limit of stiffness required for the task accomplishment. During the execution of the task the human operator receives only visual feedback of the result obtained through the Tele-Impedance based teleoperation. A six axis F/T sensor has been mounted to the peg for the assessment of the dynamic interaction forces.

IV. Results

Figure 3 shows typical results from the calibration trial using mechanical perturbations. In this graph, the displacements of the human hand along with the corresponding reaction forces are shown. Data from all similar trials were de-noised and concatenated for the estimation of the human arm endpoint impedance. The stiffness matrix (K in Eq. 3) was used for the calibration of stiffness model, as described above. Once the model

parameters were estimated and calibrated, the subject was asked to perform three different Peg-in-Hole experiments. The experiments were designed in order to explore the role of the stiffness profile during the dynamic interaction between peg and the hole, particularly its effect on the interaction forces. In the first experiment, the Cartesian stiffness of KUKA robotic arm were set to a relatively high value (K= [1200, 1200, 1200] N/m). Cartesian damping values in all experiments were set to a constant value of (D= [0.7, 0.7, 0.7] N.s/m). Following this, the subject was asked to move his hand in space and teleoperate the robot to insert the peg in the hole. The task was performed only by means of position control while the stiffness was maintained constantly high, as described above.

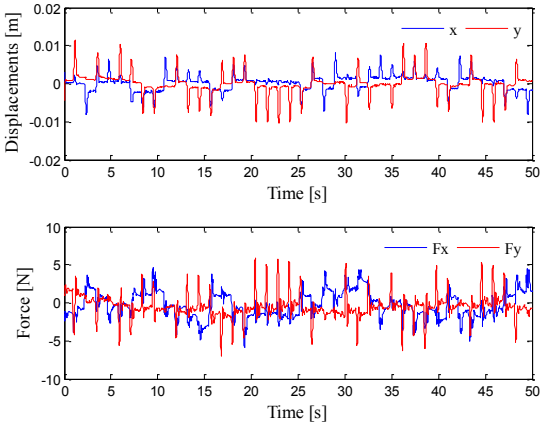

Fig. 3. Typical data obtained from a trial during the endpoint impedance estimation experiment . Exerted random displacements in x (blue) and y (red) directions (upper plot) and restoring forces (lower plot).

Figure 4.A presents the dynamic interaction forces between the surfaces of the peg and the hole, and the position tracking errors in three dimensions. As it is shown in the figure, the task is accomplished due to high values of stiffness, however, small position errors have generated relatively large forces in the corresponding directions (80N in -Z direction), once the peg starts interacting with the hole surface (t=10s). This problem overshadows safety issues both for the robot itself but also damage risks for equipments/objects handled during the execution of the task.

Figure 4.B demonstrates results from the second experiment in which the same task was executed with the KUKA, arm stiffness fixed to low values (K= [120, 120, 120] N/m). Position errors (particularly in y direction) have slightly increased in reaching phase. Once the peg is positioned around the hole space (t≈ 17.8s), the dynamic interaction forces raise, nevertheless, notably lower than the former case due to more compliant end-effector profile. Slight end-effector position adjustments, as a result of subjects hand movements align the peg with the hole. As soon as the peg was aligned with the hole the insertion phase started by simply moving the human hand in Z direction. The force at the insertion direction starts to increase; however, it is not sufficient for the accomplishment of the task due to the friction forces between the surfaces of the peg and the hole. As a consequence, KUKA's end-effector could not track the subject's vertical reference displacements and position error tends to increase in Z direction (Lower graph, green line). Once the position error increases, KUKA's controller finally triggers a fault condition by virtue of insufficient generated torque to follow the planned trajectory.

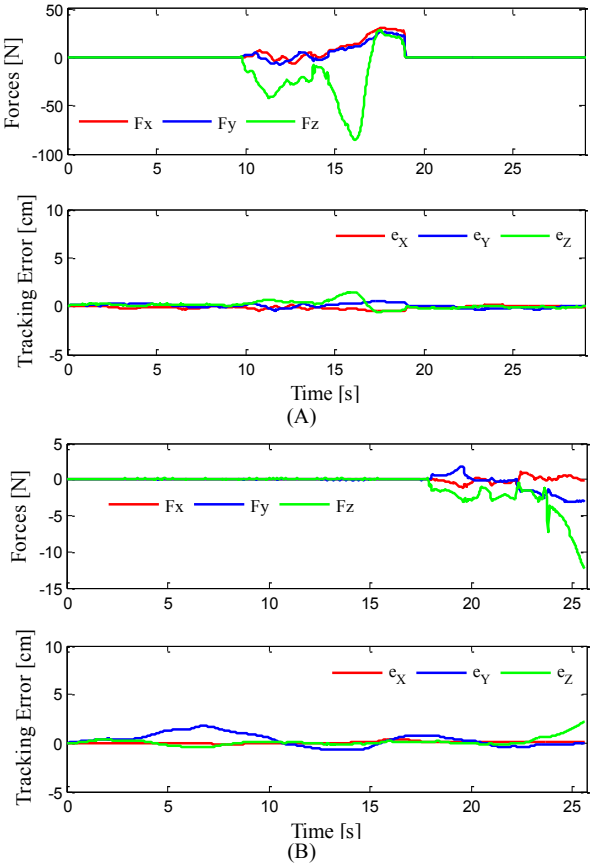

Fig. 4. Dynamic interaction forces between peg and the hole and position tracking error in x, y and z directions, with A) fixed high values of endpoint stiffness ([1200, 1200, 1200] N/m) and B) fixed low values of endpoint stiffness ([120, 120, 120] N/m).

Figures 5 and 6 demonstrate the experimental results of the Tele-Impedance trial. In this experiment the operator guides the peg to the hole area by exploiting low co-contractions. In this phase, estimated stiffness values are not valid (due to position dependency of the stiffness ellipse and dynamic behavior of the stiffness profile) but will not affect the overall guiding in the free space. This is because the free space path planning is mostly performed based on optimized trajectories descending from CNS. This optimization algorithm inherently is included in position control of the robotic arm. Once the peg reaches to the constrained environment (hole space), the operator performs co-contractions (Fig. 5) in order to increase and adjust the endpoint stiffness (Fig. 5, lower graph). Once moderate and sufficient level of stiffness to overcome the friction forces is reached, the operator moves his hand downwards till the peg is inserted into the hole. Similar stiffness levels are used in order to overcome friction and pull the peg out from the hole. As depicted in plots in figure 6, position tracking errors are acceptable and undesired deviations of the end-effector

do not cause high interaction forces as in the stiff case, particularly while sliding on the surface to find the hole space (t=17 to 22s). As mentioned, the insertion of the peg in the hole and the pull out phase are performed in the position which the parameters of the endpoint stiffness model were estimated and calibrated. Therefore, the precision of estimated stiffness profile is highly acceptable for the Peg-in-Hole task executed through the continuously adjusted Tele-Impedance control performed by the operator by means of adjusted co-contractions.

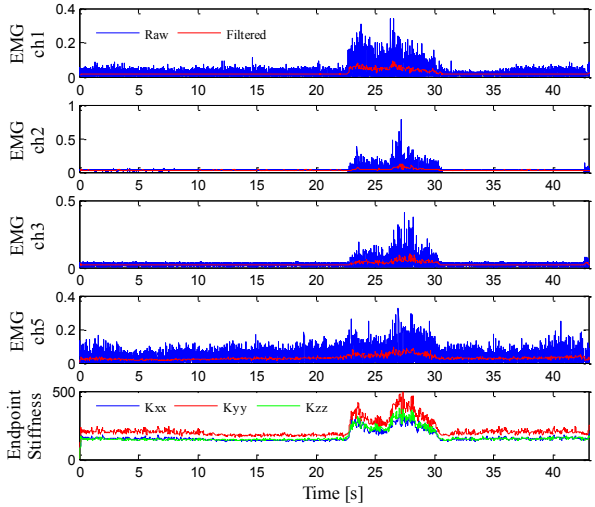

Fig. 5. Raw (blue) and filtered (red) EMG measurements of sample muscles (BRAD, TRIO, TRIM and BILH) and estimated endpoint stiffness values (bottom plot).

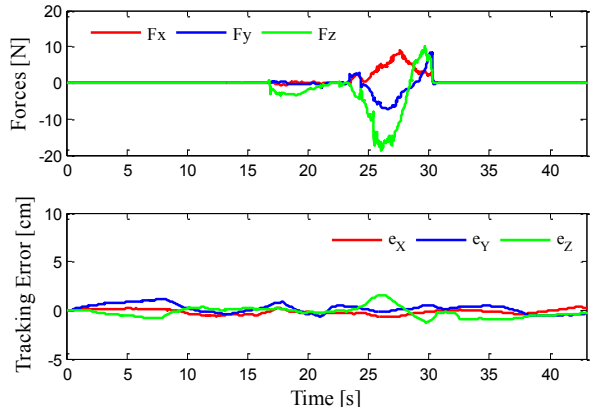

Fig. 6. Dynamic interaction forces between peg and the hole (upper graph) and position tracking error in x, y and z directions (lower graph) based on Tele-Impedance. Acceptable position tracking performance during reaching and dynamic force interactions between peg and the hole is assured.

V. Discussions and Conclusions

This work introduced the concept of Tele-Impedance, a method to effectively control/or remotely operate a robot arm. Alternatively to position based or closed loop bilateral force reflecting teleportation, the proposed approach augment the command profile sent to the robot by including apart from the position reference also the desired impedance profiles. This supplementary information can assist the robotic arm to demonstrate a versatile and stable behavior while interacting with the remote environments under the continuously modulated position/impedance command of the human operator.

The impedance (stiffness) profile sent to the robot was derived in real time from the measurement of EMGs from eight muscles of the operator arm. The stiffness of the human arm endpoint was performed using the index based model of muscle co-contractions introduced in [21]. This simplified but precise model of human endpoint stiffness has been adopted in order to give an insight to the peg-in-hole robotic problem.

The procedures used for the calibration of the model were introduced and the Tele-Impedance control concept was successfully demonstrated through the tele-execution of a traditional Peg in Hole task using the KUKA light weight arm system. In this Tele-Impedance setup the position and the estimated stiffness of the human arm endpoint (wrist) were acquired and used to continuously command the Cartesian position and stiffness of the KUKA light weight arm to perform the Peg in Hole task.

Preliminary results from these trials demonstrated the feasibility of the Tele-Impedace control and indicated its high potential in applications where the interaction between the robot and the environment needs to be controlled.

We believe that the continuous modulation of the endpoint impedance during teleoperation can finally permit robots to reach interaction performances close to those achieved by the human arm demonstrating a versatile and stable behavior even when interacting with environments with dynamic uncertainties.

References

[1] T. B. Sheridan, “Space teleoperation through time delay: Review and prognosis,” IEEE Trans. Robot. Autom., vol. 9, no. 5, pp. 592–606, 1993.

[2] B. Hannaford, “A design framework for teleoperators with kinaesthetic feedback,” IEEE Trans. Robot. Autom., vol. 5, no. 4, pp. 426–434, 1989.

[3] T. Imaida, Y. Yokokohji, T. Doi, M. Oda, and T. Yoshikawa, “Ground space bilateral teleoperation of ETS-VII robot arm by direct bilateral coupling under 7-s time delay condition,” IEEE Trans. Robot. Autom., vol. 20, no. 3, pp. 499–511, Jun. 2004.

[4] G. M. Leung, B. A. Francis, and J. Apkarian, “Bilateral controller for teleoperators with time delay via mu-synthesis,” IEEE Trans. Robot. Autom., vol. 11, no. 1, pp. 105–116, Feb. 1995.

[5] G. Niemeyer and J.-J. E. Slotine, “Telemanipulation with time delays,” Int. J. Robot. Res., vol. 23, no. 9, pp. 873–890, 2004.

[6] G. M. Leung, B. A. Francis, and J. Apkarian, “Bilateral controller for teleoperators with time delay via mu-synthesis,” IEEE Trans. Robot. Autom.,1995.

[7] W. S. Kim, B. Hannaford, and A. K. Bejczy, “Force-reflection and shared compliant control in operating telemanipulators with time delay,” IEEE Trans. Robot. Autom., vol. 8, no. 2, pp. 176–185, Apr. 1992.

[8] A. Eusebi and C. Melchiorri, “Force reflecting telemanipulators with timedelay: Stability analysis and control design,” IEEE Trans. Robot. Autom., vol. 14, no. 4, pp. 635–640, Aug. 1998.

[9] D. A. Lawrence, “Stability and transparency in bilateral teleoperation,” IEEE Trans. Robot. Autom., vol. 9, no. 5, pp. 624–637, Oct. 1993.

[10] L. J. Love and W. J. Book, “Force reflecting teleoperation with adaptive impedance control,” IEEE Trans. Syst.,Man, Cybern. B, Cybern., vol. 34, no. 1, pp. 159–166, Feb. 2004.

[11] B. Hannaford and R. Anderson, “Experimental and simulation studies of hard contact in force reflecting teleoperation,” in Proc. 1988 IEEE Int. Conf. Robot. Autom., pp. 584–589.

[12] T. Chan, S. Everett, and S. Dubey, “Variable damping impedance control of a bilateral telerobotic system,” in Proc. 1996 IEEE Int. Conf. Robot. Autom., pp. 2033–2040.
[13] N. Hogan, “Impedance control: An approach to manipulation,” Trans. ASME, J. Dyn., Syst. Meas., Control, vol. 107, pp. 1–24, Mar. 1985.
[14] A. Albu-Sch¨affer, S. Haddadin, C. Ott, A. Stemmer, T. Wimb¨ock, and G. Hirzinger, “The DLR Lightweight Robot Lightweight Design and Soft Robotics Control Concepts for Robots in Human Environments,” Industrial Robot Journal, vol. 34, pp. 376–385, 2007.
[15] A. Bicchi and G. Tonietti, “Fast and soft arm tactics: Dealing with the safety-performance trade off in robot arms design and control,” IEEE Robotics and Automation Mag., vol. 11, no. 2, pp. 22–33, 2004.
[16] A.Jafari, N.G. Tsagarakis, B. Vanderborght, and Darwin Caldwell, “AwAS: a novel actuator with adjustable stiffness,” is in the Proceeding of IEEE/RSJ International Conference on Intelligent Robots and Systems (IROS), 2010, pp. 4201-4206.
[17] G. Tonietti, R. Schiavi, and A. Bicchi, “Design and control of a variable stiffness actuator for safe and fast physical human/robot interaction,” in Robotics and Automation, 2005. ICRA 2005. Proceedings of the 2005 IEEE International Conference on, 2005, pp. 526–531.
[18] S. Wolf and G. Hirzinger, “A new variable stiffness design: Matching requirements of the next robot generation,” in IEEE International Conference on Robotics and Automation (ICRA 2008), May 2008, pp. 1741–1746.
[19] E. Bizzi, N. Accornero, W. Chapple, and N. Hogan, “Posture control and trajectory formation during arm movement”. J Neuroscience, vol. 4, pp. 2738–2744, 1984.
[20] M. Kawato, K. Furukawa, and R. Suzuki, “A hierarchical neural-network model for control and learning of voluntary movement”. Biol Cybern. vol. 57, pp. 169–185, 1987.
[21] R. Osu, DW. Franklin, H. Kato, H. Gomi, K. Domen, T. Yoshioka, and M. Kawato, “Short- and long-term changes in joint co-contraction associated with motor learning as revealed from surface EMG”. J Neurophysiol. vol. 88, pp. 991–1004, 2002.
[22] JM. Dolan, MB. Friedman, ML. Nagurka, “Dynamic and loaded impedance components in the maintenance of human arm posture”. IEEE Trans Systems Man Cybern. vol. 23, pp. 698–709, 1993.
[23] T. Tsuji, PG. Morasso, K. Goto, and K. Ito, “Human hand impedance characteristics during maintained posture”. Biol Cybern. vol. 72, pp. 475– 485, 1995.
[24] P. K. Artemiadis and K. J. Kyriakopoulos, "EMG-based position and force control of a robot arm: Application to teleoperation and orthosis," in Proceedings of IEEE/ASME International Conference on Advanced Intelligent Mechatronics, pp. 1-6, 2007.
[25] C. Castellini and P. van der Smagt, “Surface EMG in advanced hand prosthetics”. Biological Cybernetics, 2006.
[26] H. Gomi and R. Osu, “Task-Dependent Viscoelasticity of Human Multi joint Arm and Its Spatial Characteristics for Interaction with Environments”. J Neurosci., vol. 18, pp. 8965-78, 1998.
[27] F. A. Mussa-Ivaldi, N. Hogan, and E. Bizzi, “Neural, mechanical, and geometric factors subserving arm posture in humans,” J. Neurosci., vol. 5, no. 10, pp. 2732–2743, 1985.
[28] G. Schreiber, A. Stemmer, and R. Bischoff, “The Fast Research Interface for the KUKA Lightweight Robot”. In IEEE International Conference on Robotics and Automation, 2010.
[29] A. Albu-Schäffer, Ch. Ott, and G. Hirzinger “A unified passivity-based control framework for position, torque and impedance control of flexible joint robots”, in Int. Journal of Robotics Research, vol. 26, no. 1, pp. 23–39, 2007.